Early results of the image reconstruction problem from STIX data

Massa P. [1] Perracchione E. [1,2] Garbarino S. [1] Battaglia A. F. [4,5] Benvenuto F. [1] Massone A. M. [1] Piana M. [1,2] Hurford G. J. [4] Krucker S. [3,4]

[1]MIDA, Dipartimento di Matematica, Università degli Studi di Genova, Genova, Italy [2]CNR-SPIN, Genova, Italy [4]Space Sciences Laboratory, University of California, Berkeley, USA

[4]University of Applied Sciences and Arts Northwestern Switzerland, Windisch, Switzerland [5]Swiss Federal Institute of Technology in Zurich (ETHZ), Zurich, Switzerland

The Spectrometer/Telescope for Imaging X-rays (STIX)

The Spectrometer/Telescope for Imaging X-rays (STIX) [1] is the hard X-ray telescope of the Solar Orbiter mission conceived for the measurement of hard X-ray photons emitted by thermal and non-thermal mechanisms during solar flares. The imager consists of 32 subcollimators (i.e. couples of grids mounted in front of a detector). Among them:

- 30 are used for imaging;
- one provides a coarse estimate of the source location (Coarse Flare Locator);
- one is used for monitoring the background radiation.

In each of the 30 subcollimators used for imaging, the rear and the front grid have different orientation and pitch and their superimposition gives rise to a Moiré pattern on the detector surface (see figure 1). This pattern is sensitive to the flaring source location and morphology. From the measurements of amplitude and phase of the Moiré patterns, it is possible to compute the value of 30 Fourier components of the angular distribution of the source, named **visibilities**.

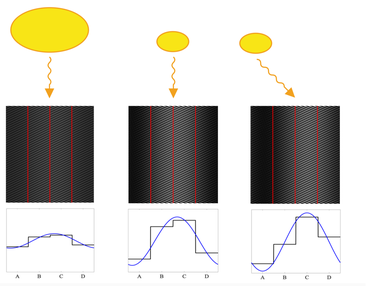

Figure 1:Moiré patterns corresponding to sources with different size and location. The amplitude of the pattern (i.e. the difference between the maximum and the minimum) is sensitive to the source size, while the phase of the pattern (i.e. the location of the peak of the pattern) is sensitive to the source location.

The image reconstruction problem for STIX is then the one of inverting the Fourier transform of the sought signal from limited data.

Image reconstruction problem from STIX visibility amplitudes

The STIX data calibration is completed just for the visibility amplitudes. However, the visibility phase calibration is close to the end and preliminary results about imaging from fully-calibrated data are shown in this poster. For an initial validation of STIX imaging capabilities it has been necessary to solve the image reconstruction problem from visibility amplitudes, described by the equation

$$|\mathcal{F}\varphi| = |V| \,, \tag{1}$$

where φ is the image of the flaring source to reconstruct, $V = (v_1, \ldots, v_{30})$ is the array of the visibilities, $\mathcal{F}$ is the Fourier transform computed in the angular frequencies sampled by STIX and $|\cdot|$ is applied component-wise. Problem (1) is nonlinear; moreover, the visibility amplitudes contain information only on dimension, orientation and relative position of the sources, but not on the absolute location of the flare. Given that, we addressed (1) by using **parametric source shapes** and by retrieving their parameters by means of **forward fitting techniques** [2]. Specifically, the parametric shapes we used are (see figure 2):

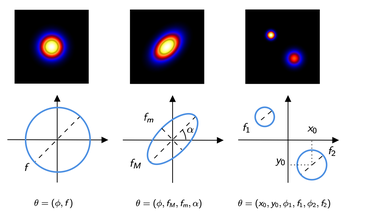

Figure 2:Parametric source shapes

- a Gaussian circular source, parameterized by the total flux ϕ and the Full Width at Half Maximum (FWHM) f;
- a Gaussian elliptical source, parameterized by the total flux ϕ, the minimum and maximum FWHM f_m, f_M and the orientation angle α;
- a double Gaussian circular source, parameterized by the total flux of the two sources ϕ_1, ϕ_2, the FWHM of the two sources f_1, f_2 and coordinates of the center of one source (x_0, y_0) (the other source is symmetric with respect to the origin).

Amplitude-based methods

For retrieving the source parameters from the visibility amplitudes, we implemented two forward fitting methods. The first is based on Particle Swarm Optimization (PSO) and it solves the following optimization problem:

$$\arg\min_{\theta \in \mathcal{D}} \chi^2(\theta) \,, \tag{2}$$

where θ is the array of parameters of a chosen parametric shape, $\mathcal{D}$ is the so-called feasibility region for θ and $\chi^2(\theta)$ measures the square of the discrepancy between the experimental visibility amplitudes and those predicted by computing the Fourier transform of the source shape parameterized by θ. Uncertainty quantification with PSO is realized by perturbing the data multiple times with Gaussian noise and by computing the standard deviation of the parameter values obtained by solving (2) from the perturbed data. The second method is based on Sequential Monte Carlo and it provides the posterior probability distribution on θ given the observed visibility amplitudes. For the sake of brevity, in this poster we present just the results obtained with PSO (see [2] for a detailed comparison of the two methods).

Image reconstruction problem from calibrated STIX data

The image reconstruction problem from calibrated STIX data is the linear problem of determining the image of the solar flare φ that satisfies

$$\mathcal{F}\varphi = V \,. \tag{3}$$

The imaging problem (3) is completely analogous to the one of the Reuven Ramaty High Energy Solar Spectroscopic Imager (RHESSI). Therefore, its solution can be addressed with algorithms already implemented for that instrument, such as the maximum entropy method MEM_GE [3].

Results: May 2021 flares

We validate the results of the STIX image reconstruction problem both from visibility amplitudes and from calibrated data on two different events recorded on May 7 2021 in the time interval 18:51:00-18:53:40 UT and on May 9 2021 in the time interval 13:53:10-13:55:00 UT.

In the first row of figure 3 we show the May 7 2021 event from the Solar Orbiter vantage point (left panel) and from the Earth vantage point (right panel). For comparison, we overlay the STIX reconstruction from fully-calibrated data (left panel) and the Hinode/XRT map (right panel) on the 1600 Å map provided by the Atmospheric Imaging Assembly (AIA) of the Solar Dynamics Observatory. We point out that the AIA map in the left panel has been rotated in order to keep into account the different vantage point of Solar Orbiter with respect to the one of AIA. Moreover, the STIX reconstruction, obtained with MEM_GE, has been shifted of about 50 arcsec as determining the absolute position of the source with higher accuracy is still part of the calibration process. A comparison of the reconstructions obtained from STIX visibility amplitudes (with PSO) and from fully-calibrated data is shown in the second row of figure 3 in the case of the May 7 2021 event. As the non-thermal emission is clearly composed by two Gaussian-shaped footpoints, PSO gives good results in terms of orientation and separation between the reconstructed footpoints. Finally, we performed the same comparison between the PSO reconstruction and the MEM_GE one in the case of the May 9 2021 event (third row of figure 3). Even if the position of the flare ribbons (shown by the AIA 1600 Å map) is inside the error bars on the footpoint locations provided by PSO, the orientation of the non-thermal emission obtained from visibility amplitudes is not accurate in this case. This result shows the limitations of a parametric method when the shape used for fitting is not similar to the real one. Indeed, with the non-parametric method MEM_GE we obtain good performances in terms of dimension, orientation and shape of the reconstructed non-thermal emissions when compared to the AIA map.

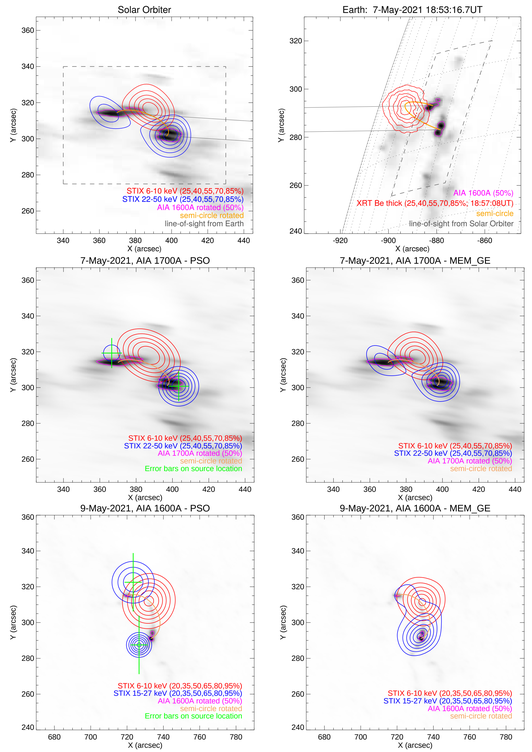

Figure 3:First row: May 7 2021 event from the Solar Orbiter vantage point (left) and from the Earth vantage point (right). The MEM_GE reconstruction and the XRT map are overlayed to the AIA 1600 Å map (left and right panel, respectively). Second row: May 7 2021 event reconstructed by PSO (left) and by MEM_GE (right). Third row: May 9 2021 event reconstructed by PSO (left) and by MEM_GE (right).

Conclusions

We presented the image reconstruction problem from STIX data and we validated the results obtained both from visibility amplitudes and from fully-calibrated data on two events recorded in May 2021. Even if amplitude imaging has been useful during the calibration process to check the STIX imaging capabilities, it gives suboptimal results when the parametric source shape used for fitting the data does not reflect the real geometry of the flare. Finally, we showed the first results from fully calibrated data proving that the reconstructions are reliable in terms of dimension, orientation and shape when compared to the corresponding AIA maps.

References

[1] Krucker S., Hurford G. J., Grimm O. et al. (2020), A&A, 642, A15

[2] Massa, P., Perracchione, E., Garbarino, S., et al. (2021), accepted (A&A)

[3] Massa, P., Schwartz R., Tolbert A. K., et al. (2020), ApJ, 894, 46